Nanoparticle Tracking

DOI: 10.1002/anie.201202340

Determining the Full Three-Dimensional Orientation of Single Anisotropic Nanoparticles by Differential Interference Contrast Microscopy**

*Lehui Xiao, Ji Won Ha, Lin Wei, Gufeng Wang, and Ning Fang**

Plasmonic gold nanorods (AuNRs) have been used as orientation probes in optical imaging because of their shape-induced anisotropic optical properties.[1] However, current optical imaging techniques lack the capability to decipher the full three-dimensional (3D) orientation of an in-focus gold nanorod in the four quadrants of the cartesian plane. Resolving the orientation angles and determining the accurate rotational modes of the gold nanorod are critical in biological observations because the chirality of biological macromolecules and their assemblies, for example right- or left-handed helices, is fundamental in biology. Herein, we overcome this limitation by combining differential interference contrast (DIC) microscopy image pattern recognition with DIC polarization anisotropy analysis to resolve the exact azimuthal angles (from 0° to 360°) as well as the polar angles of tilted AuNRs that are positioned in the focal plane of the objective lens without sacrificing the spatial and temporal resolution. The rotational direction of individual in-focus AuNRs can thus be tracked dynamically. Finally, we successfully monitored the real-time rotational behavior of transferrin-modified gold nanorods on live cell membranes.

Many biological processes involve rotational motion at the nanoscale, for example RNA folding,[2] walking of molecular motors,[3] twisting of dynamin assembly,[4] and self-rotation of ATPase.[5] Tracking the rotational motion with optical probes is of great importance to understanding these processes in biological and engineered environments. Fluorescence anisotropy has been commonly attempted to probe the rotational motion of biomolecules using organic dyes, conjugated polymers, and inorganic semiconductor nanocrystals.[6] Nevertheless, the major disadvantages of current fluorescent orientation probes are stochastic transition between on and off states,[7] high photobleaching tendency,[7a,8] and less-than-desirable biocompatibility,[9] thus limiting their use in biological systems.

Recently, AuNRs have gained considerable attention as suitable orientation probes because of their shape-induced anisotropic optical properties,[1a–c] large scattering and absorption cross-sections resulting from the surface plasmon resonance (SPR) effect, high chemical and photostability, and excellent biocompatibility.[10] Scattering- and absorption-based polarization anisotropy measurements of AuNRs have been carried out under dark-field (DF) microscopy[1a] and photothermal heterodyne imaging.[1d] These methods were successfully used to measure the orientation of AuNRs. However, in these methods, only the in-plane orientation is effectively obtained while the out-of-plane orientation is still ambiguous. Furthermore, their applicability for studies of fast dynamics in live cells is limited. It is a challenge for DF microscopy to differentiate AuNRs from other highly scattering cellular components. Photothermal heterodyne imaging requires rapid scanning of the sample to collect an image and comprehensive intensity and polarization modulation of the heating beam.

DIC microscopy is better suited to probe orientation and rotational motion of nanoobjects in live cells when used in combination with plasmonic AuNRs.[1e] DIC microscopy resolves the optical path difference between two mutually orthogonally polarized beams separated by a shear distance along the optical axis of a Nomarski prism (Supporting Information, Figure S1). The nature of the interference makes it insensitive to the scattered light from surrounding cellular components and keeps its high-throughput capability. Therefore, the DIC microscopy-based single particle orientation and rotational tracking (SPORT) technique is more applicable to the studies of fast rotational dynamics in live cells.

When plasmonic nanoparticles are illuminated under an optical microscope, the incident electromagnetic wave is commonly attenuated through absorption and scattering.[11] The attenuation at a given wavelength is quantified by the corresponding cross-section. Typically, when a AuNR is excited by monochromatic light at the longitudinal SPR wavelength, the scattered electromagnetic field can be simplified as generated from a single dipole with the oscillation direction along its principal axis, provided that the nanorod is much smaller than the wavelength of light.[11]

[*] Dr. L. Xiao,[+] J. W. Ha,[+] L. Wei, Dr. G. Wang, Prof. N. Fang
Ames Laboratory, U.S. Department of Energy, and Department of Chemistry, Iowa State University
Ames, IA 50011 (USA)
E-mail: nfang@iastate.edu
Dr. L. Xiao,[+] L. Wei
Biomedical Engineering Center, State Key Laboratory of Chemo/Biosensing and Chemometrics, College of Chemistry and Chemical Engineering, Hunan University
Changsha, 410082 (P.R. China)

[+] These authors contributed equally to this work.

[**] This work was supported by the U.S. Department of Energy, Office of Basic Energy Sciences, Division of Chemical Sciences, Geosciences, and Biosciences through the Ames Laboratory. The Ames Laboratory is operated for the U.S. Department of Energy by Iowa State University under contract no. DE-AC02-07CH11358. L.X. expresses thanks for the partial support from the Scholarship Award for Excellent Doctoral Student from the Ministry of Education, China.

Supporting information for this article is available on the WWW under http://dx.doi.org/10.1002/anie.201202340.

The DIC image of AuNR is resulted from the interference of two mutually shifted, phase-delayed, and orientation-dependent scattering images. Quantitatively, the relative bright and dark intensities of AuNR can be simplified into Equation (1) (for details, see the Supporting Information):

$$I_B - I_0 \propto \cos^2(\phi)\sin^2(\theta)$$
$$I_0 - I_D \propto \sin^2(\phi)\sin^2(\theta) \quad (1)$$

where I_0 is the background intensity, I_B and I_D are the bright and dark intensities, respectively, and ϕ and θ are the azimuthal and polar angles as defined in Figure 1 A. The bright and dark intensities are the projections of the dipole onto the bright and dark polarization directions, respectively. Therefore, the angular-dependent DIC intensities can be used to extract the information on the orientation of the AuNRs. The DIC polarization anisotropy P, which is defined in Equation (2),[12] can be conveniently computed from the orthogonally polarized bright and dark intensities in a DIC image at the longitudinal SPR wavelength:

$$P = \frac{I_{B,N} - I_{D,N}}{I_{B,N} + I_{D,N}} \quad (2)$$

where $I_{B,N}$ and $I_{D,N}$ are normalized relative bright and dark intensities [Eq. (1)], respectively. Obviously, the DIC polarization anisotropy is only dependent on the azimuthal angle of ϕ, while the sum value of the relative bright and dark intensities is purely related with the polar angle of θ. By determining the DIC polarization anisotropy and sum value of the bright and dark parts from the DIC image, the rotational dynamics of individual AuNR then could be readily quantified. Further error estimation for the azimuthal and polar angle determination based on the above calculations is shown in the Supporting Information, Figure S2.

The angular degeneracy for a AuNR is currently the major challenge of the previously reported DIC microscopy-based technique[1e,12] as well as other polarization-based techniques for resolving the exact 3D orientation of AuNRs in the focal plane of the objective lens. In the previous study,[1e] we used the absolute bright and dark intensities directly to determine the AuNR orientation, which could only resolve the orientation angle from one of the four quadrants, that is, from 0° to 90°. Furthermore, although the DIC polarization anisotropy using an intensity ratio instead of absolute intensities provides a more reliable and accurate angle measurements of a AuNR in dynamic studies, it still cannot distinguish those mirror orientation angles (that is, ϕ, $\pi-\phi$, $\pi+\phi$, and $2\pi-\phi$ have the same DIC polarization anisotropy value) with respect to the polarization directions of a AuNR.[12,13] Therefore, it is not feasible to rapidly distinguish the ambiguous rotational motions, such as clockwise or counterclockwise, of a AuNR in the focal plane. However, the rotational direction is important to unveil the underlying mechanisms of many biological processes, as chiral biological macromolecules and their assemblies, for example right- or left-handed helices, are involved.

In the present study, we overcome the limitation described above by combining DIC image pattern recognition with DIC polarization anisotropy measurement. We demonstrate that the full 3D orientation information can be extracted for in-focus AuNRs that are tilted with respect to the horizontal object plane. The light scattered by a tilted anisotropic AuNR has a skewed electromagnetic field distribution containing full-space angular information, which, however, is not resolvable in a single focused fluorescence or DF image. Thus, defocused orientation imaging techniques have been employed to determine 3D orientations of out-of-focus nanoprobes within a single frame.[1b,3,14] The defocused imaging techniques are based on the electric dipole approx-

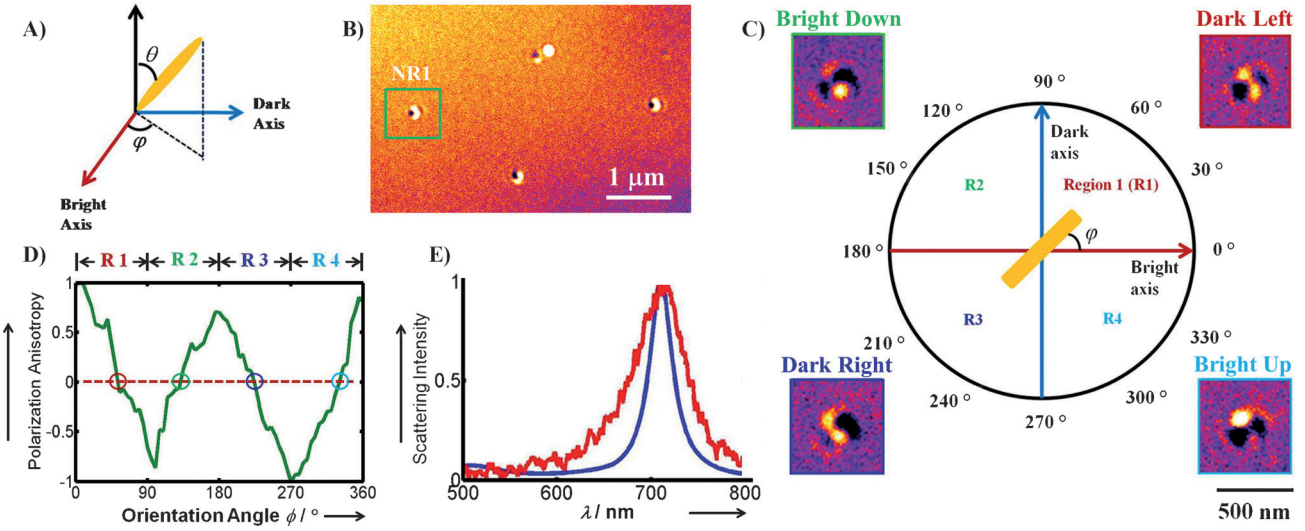

Figure 1. Orientation of a AuNR that is tilted in gel matrix with a polar angle of about 14°. A) Azimuthal angles ϕ and polar angles θ in cartesian coordinates. B) DIC image under 700 nm illumination. C) Changes in DIC image patterns of AuNR1 highlighted in (B) as a function of azimuthal angle. Four different image patterns appear for the tilted AuNR1: the dark part on the left (R1), bright part down (R2), dark part right (R3), and bright part up (R4). D) DIC polarization anisotropy P for AuNR1 (green curve) as a function of azimuthal angle ϕ. The dotted line is drawn at $P=0$ and there are four points of contact at this P value. The corresponding images at each point of contact for four frames at $P=0$ are shown in (C). E) The measured (red) and simulated (blue) scattering spectra of AuNR1.

imation and the fact that the dipole radiation exhibits an angular anisotropy. When a nanoprobe is positioned outside of the focal plane, the intensity distribution of the blurred image provides information about the emission dipole orientation of the nanoprobes; however, the standard defocused imaging technique does not always yield orientation accurately owing to largely reduced signal intensity. Furthermore, it is usually required to switch back and forth between focused and defocused imaging for obtaining the orientation and localization information simultaneously with precision, which sacrifices the temporal resolution in dynamic tracking experiments. As demonstrated by Toprak et al., the temporal resolution was only 1–2 frames per second (fps) owing to the much reduced signal intensity from the defocused imaging mode.[3] Therefore, the standard defocused imaging strategy is more suitable for the characterization of static events. On the contrary, in DIC microscopy, the final image is generated from the interference of two mutually shifted, phase-delayed, and orientation-dependent scattering images. Thus, the electromagnetic field distribution is artificially encoded into the DIC point spread function, resulting in identifiable orientation-dependent DIC image patterns for AuNRs in the focal plane. To demonstrate this, we studied the DIC images of tilted AuNRs (25 nm × 73 nm) embedded in 2% agarose gel matrix. The polar angle θ of AuNR 1 (Figure 1B) was first determined to be 14° by using the defocused DF imaging technique (Supporting Information, Figure S3).[1b] We then obtained the corresponding DIC images of the same AuNRs at 700 nm excitation (Figure 1B). A 360° rotation study was carried out by rotating the stage by 5° per step to position AuNR 1 in different orientations. The exact focal plane of the AuNR was found by scanning in the z direction with a vertical step size of 69 nm. Based on the positions and intensities of the bright and dark parts in each frame, four distinctive image patterns are found to represent the nanorod orientations in the four quadrants (R1 to R4) of the cartesian plane (Figure 1C). The complete set of DIC images of AuNR 1 at 72 orientations from 0° to 360° with an interval of 5° are shown in the Supporting Information, Figure S4. The normalized bright and dark DIC intensities for AuNR 1 can be fitted well with the functions in Equation (1) (Supporting Information, Figure S5), thus indicating the good reliability of the dipole approximation applied in this work. Figure 1D shows a plot of the polarization anisotropy as a function of frame for AuNR 1.

The DIC image patterns of AuNRs change as a function of orientation angle because the spatial distribution of the scattered electromagnetic field from AuNRs is closely related to the orientation angles of AuNRs. The light scattered by the tilted AuNR 1 is projected onto slightly different positions on the DIC images after interference to generate different image patterns. The trend in the pattern changes for AuNR 1 is consistent with other AuNRs that are tilted. To further confirm AuNR 1 was a single nanoparticle instead of an aggregate, we determined its scattering spectrum with a transmission grating beam splitter with 70 lines per mm in front of the Hamamatsu complementary metal oxide semiconductor (CMOS) camera in DF mode. This transmission grating allowed one portion of the incoming scattering light to form the zeroth-order image and dispersed another portion of the light to form the wavelength-resolved first-order image. Both the zeroth-order and first-order images can be captured by the camera. The measured longitudinal SPR peak of AuNR 1 appears at 708 nm, which agrees well with the simulated spectrum (Figure 1E). The demonstrated ability to readily distinguish the orientations in the four quadrants (R1 to R4) using the DIC image patterns allows us to resolve the exact azimuthal angle (from 0° to 360°) of an in-focus AuNR in a single DIC image by combining with DIC polarization anisotropy measurement. It is worth noting that the DIC image pattern recognition is only used to identify the exact quadrant in which the AuNR is located. Thus, the strategy of integrating the pattern recognition technique and DIC polarization anisotropy is principally more reliable and accurate than the previously demonstrated standard defocused imaging methods, which are based solely on matching the measured image pattern with a set of simulated defocused PSFs.

Further investigation revealed that the distinctively different DIC image patterns can only be generated for AuNRs that are tilted (neither totally lying flat on the horizontal plane nor standing straight up along its long axis) in the 3D space. For the AuNRs that were set flat on a pre-cleaned glass slide by spin casting, the bright and dark DIC intensities are also changed periodically as it rotates from 0° to 360° (Supporting Information, Figure S6 and S7) and show good fits to the functions in Equation (1) (Supporting Information, Figure S8). However, these image patterns are similar in all four quadrants. The difference in image patterns increases as the polar angle θ decreases from 90°, and the cutoff polar angle θ to show sufficient difference is estimated to be 70° (Supporting Information, Figure S9).

To further demonstrate the usefulness of this technique, we tracked rotational dynamics of AuNRs on live cell membranes. Functional AuNRs are considered efficient delivery cargoes in biological applications.[10] Tracking rotational and translational dynamics of individual AuNRs on live cell membranes will lead to a better understanding of drug delivery mechanisms and other cellular processes, such as endocytosis.[15] In this regard, transferrin-modified AuNRs rotating on live cell membranes were chosen as a model system to verify the applicability of this method toward resolving fast rotational dynamics in biological systems.

We recorded image stacks that show rotational motions of a AuNR (AuNR 2) on a live cell membrane at a temporal resolution of 100 ms (Figure 2A). On the fluidic and uneven cell membrane, AuNR 2 was more often tilted to give rise to the required image patterns for azimuthal orientation identification within 0–360°. 30 consecutive frames (Figure 2B) were chosen from a movie that displays clear transitions among different image intensities and patterns when AuNR 2 was tilted. DIC polarization anisotropy was computed for the 30 images to extract the azimuthal angle ϕ. Based on the pattern recognition technique, then the DIC image patterns were used to resolve the true orientation angle ϕ in the four quadrants. Finally, the sum value of the bright and dark parts was used to determine the polar angle θ (Figure 2C). As illustrated in the polar plot of Figure 2D, in frames 1–11,

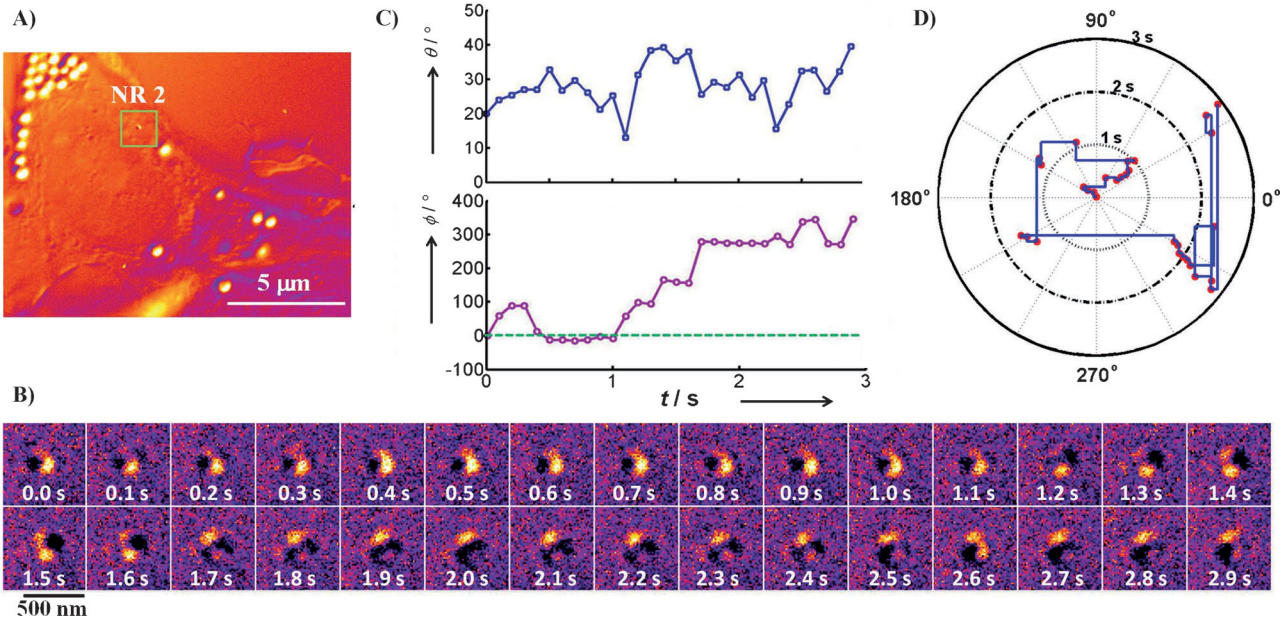

Figure 2. Dynamic rotational movements of single AuNR on a live cell membrane. A) DIC image of the live cell and AuNR2. B) 30 consecutive images of AuNR2 chosen from a movie. C) Determined relatively rotated azimuthal angle ϕ and polar angle θ for AuNR2 throughout the 30 consecutive frames. D) The rotational track of the azimuthal angle ϕ as a function of time for the image sequence of (B).

AuNR2 experienced reversible rocking motion between R1 and R2. In frame 12, it rotated to R2 and showed a continuous anticlockwise rotation until frame 27. A reminiscent rocking motion was shown again thereafter. It is worth noting that this angular rotational information only could be resolved by the methodology with full 3D angular resovability.

In summary, a novel optical rotational tracking method with the capability of full-space orientation resolvability for individual in-focus nanoprobes without sacrificing spatial and temporal resolution was demonstrated to overcome the limitations of current polarization anisotropy techniques. The applicability and usefulness of our method toward in vivo studies in biological systems was also verified by the precise tracking of 3D orientation angles of AuNRs rotating on live cell membranes. Deciphering the full 3D orientation information of the probe or nanocargo in a dynamic fashion will shed new light on physical and biological processes with characteristic rotational motions, such as the detailed working mechanisms of molecular nanomachines and relevant assisting proteins during the internalization of functional drug delivery vectors.[3,4] Using this method, further studies to elucidate the comprehensive interaction mechanisms between the functionalized nanocargoes and the membrane receptors in live cells are underway. Detailed in situ conformational information on how they bind on the cell membrane and how they move and rotate during the endocytosis process in live cells at single particle level would provide new avenues for the development of new generation of high efficient drug and gene delivery carriers.[15b,16]

Received: March 24, 2012
Revised: April 30, 2012
Published online: June 26, 2012

Keywords: gold · microscopy · nanorods · rotational tracking · single-particle tracking

[1] a) C. Sönnichsen, A. P. Alivisatos, *Nano Lett.* **2005**, *5*, 301–304; b) L. Xiao, Y. X. Qiao, Y. He, E. S. Yeung, *Anal. Chem.* **2010**, *82*, 5268–5274; c) L. Xiao, Y. Qiao, Y. He, E. S. Yeung, *J. Am. Chem. Soc.* **2011**, *133*, 10638–10645; d) W. S. Chang, J. W. Ha, L. S. Slaughter, S. Link, *Proc. Natl. Acad. Sci. USA* **2010**, *107*, 2781–2786; e) G. Wang, W. Sun, Y. Luo, N. Fang, *J. Am. Chem. Soc.* **2010**, *132*, 16417–16422.
[2] X. Zhuang, L. E. Bartley, H. P. Babcock, R. Russell, T. Ha, D. Herschlag, S. Chu, *Science* **2000**, *288*, 2048–2051.
[3] E. Toprak, J. Enderlein, S. Syed, S. A. McKinney, R. G. Petschek, T. Ha, Y. E. Goldman, P. R. Selvin, *Proc. Natl. Acad. Sci. USA* **2006**, *103*, 6495–6499.
[4] A. Roux, K. Uyhazi, A. Frost, P. De Camilli, *Nature* **2006**, *441*, 528–531.
[5] T. Nishizaka, K. Oiwa, H. Noji, S. Kimura, E. Muneyuki, M. Yoshida, K. Kinosita, Jr., *Nat. Struct. Mol. Biol.* **2004**, *11*, 142–148.
[6] J. N. Forkey, M. E. Quinlan, Y. E. Goldman, *Prog. Biophys. Mol. Biol.* **2000**, *74*, 1–35.
[7] a) W. E. Moerner, M. Orrit, *Science* **1999**, *283*, 1670–1676; b) M. Nirmal, B. O. Dabbousi, M. G. Bawendi, J. J. Macklin, J. K. Trautman, T. D. Harris, L. E. Brus, *Nature* **1996**, *383*, 802–804.
[8] X. S. Xie, R. C. Dunn, *Science* **1994**, *265*, 361–364.
[9] A. M. Derfus, W. C. W. Chan, S. N. Bhatia, *Nano Lett.* **2004**, *4*, 11–18.
[10] C. J. Murphy, A. M. Gole, J. W. Stone, P. N. Sisco, A. M. Alkilany, E. C. Goldsmith, S. C. Baxter, *Acc. Chem. Res.* **2008**, *41*, 1721–1730.
[11] C. F. Bohren, D. R. Huffman, *Absorption and scattering of light by small particles*, Wiley, New York, **1983**.
[12] J. W. Ha, W. Sun, G. Wang, N. Fang, *Chem. Commun.* **2011**, *47*, 7743–7745.
[13] J. W. Ha, W. Sun, A. Stender, N. Fang, *J. Phys. Chem. C* **2012**, *116*, 2766–2771.

[14] a) M. Böhmer, J. Enderlein, *J. Opt. Soc. Am. B* **2003**, *20*, 554 – 559; b) J. Enderlein, M. Böhmer, *Opt. Lett.* **2003**, *28*, 941 – 944; c) M. A. Lieb, J. M. Zavislan, L. Novotny, *J. Opt. Soc. Am. B* **2004**, *21*, 1210 – 1215.
[15] a) H. Ewers, A. E. Smith, I. F. Sbalzarini, H. Lilie, P. Koumoutsakos, A. Helenius, *Proc. Natl. Acad. Sci. USA* **2005**, *102*, 15110 – 15115; b) L. Xiao, L. Wei, C. Liu, Y. He, E. S. Yeung, *Angew. Chem.* **2012**, *124*, 4257 – 4260; *Angew. Chem. Int. Ed.* **2012**, *51*, 4181 – 4184.
[16] X. Shi, A. von dem Bussche, R. H. Hurt, A. B. Kane, H. Gao, *Nat. Nanotechnol.* **2011**, *6*, 714 – 719.

